Locally resonant surface acoustic wave band gaps in a two-dimensional phononic crystal of pillars on a surface

Abdelkrim Khelif
Institut FEMTO-ST, Université de Franche-Comté, CNRS, 32 Avenue de l'Observatoire, 25044 Besançon Cedex, France and International Joint Laboratory GeorgiaTech, CNRS, UMI 2958, 2-3 rue Marconi, 57070 Metz, France

Younes Achaoui, Sarah Benchabane, and Vincent Laude
Institut FEMTO-ST, Université de Franche-Comté, CNRS, 32 Avenue de l'Observatoire, 25044 Besançon Cedex, France

Boujamaa Aoubiza
Laboratoire de Mathématiques, Université de Franche-Comté, Route de Gray, 25030 Besançon Cedex, France
(Received 18 January 2010; published 10 June 2010)

We investigate theoretically the propagation of acoustic waves in a two-dimensional array of cylindrical pillars on the surface of a semi-infinite substrate. Through the computation of the band structure of the periodic array and of the transmission of waves through a finite length array, we show that the phononic crystal can support a number of surface propagating modes in the nonradiative region of the substrate, or sound cone, as limited by the slowest bulk acoustic wave. The modal shape and the polarization of these guided modes are more complex than those of classical surface waves propagating on a homogeneous surface. Significantly, an in-plane polarized wave and a transverse wave with sagittal polarization appear that are not supported by the free surface. In the band structure, guided modes define band gaps that appear at frequencies markedly lower than those expected from the Bragg interference condition. We identify them as originating from local resonances of the individual cylindrical pillars and show their dependence on the geometrical parameters, in particular with the height of the pillars. The transmission of surface acoustic waves across a finite array of pillars shows the signature of the locally resonant band gaps for surface modes and their dependence on the symmetry of the source and its polarization. Numerical simulations are performed by using the finite element method and considering silicon pillars on a silicon substrate.

DOI: 10.1103/PhysRevB.81.214303 PACS number(s): 43.20.+g, 43.35.+d, 77.65.Dq

I. INTRODUCTION

Recently, a great deal of work has been devoted to the study of phononic crystals constituted by a periodic repetition of inclusions in a matrix background. Phononic crystals[1–5] are for acoustic waves in fluids or elastic waves in solids the analogs of photonic crystals for optical or electromagnetic waves.[6,7] Several classes of phononic crystals exist and differ mainly by the physical nature of the inclusions and of the matrix. Among them, solid/solid, fluid/fluid, and mixed solid/fluid composite systems have received attention. These composite media typically exhibit stop bands in their transmission spectra, for which the propagation of sound or vibration can be strictly forbidden in all directions. The location and the width of acoustic band-gaps result from the choice of the lattice, of the shape of the inclusions, and of the constitutive materials. Using the band gap principle, the phononic crystals allow the propagation of elastic or acoustic waves to be regulated. In other words, they play the role of perfect mirrors for elastic or acoustic waves in the frequency range of the band gap. The fundamental interest of controlling the elastic energy and the potential applications of phononic crystal is well established. Indeed, the phononic band gaps can be used to filter, confine, or guide acoustic energy, and hence can be used in a variety of applications including wireless communications and sensing. Acoustic and elastic wave propagation in various phononic crystals have been studied, including bulk waves in finite structures,[8,9] surface wave on semi-infinite media,[10–14] and guided waves in slabs.[15–21] More recently, low-frequency gaps and waveguiding in a phononic crystal constituted of cylindrical dots deposited on homogeneous slab were demonstrated.[22,23] However, the effect of the rods as local resonators interacting with the slab modes did not appear clearly. In fact, when the thickness of the slab is same order of the period of the structure the presence of the antisymmetric mode at low frequency reduces significantly the nonradiative zone in the dispersion diagram of the phononic slab, as compared to the semi-infinite case.

Band gaps can originate from the Bragg reflections resulting from the periodicity of the structure. In this case, the spatial period of the crystal is of the same order of magnitude as the acoustic wavelength at the central frequency of the gap. Most of the works in the literature were based on Bragg reflection and as a consequence the lattice constant has generally been the key parameter to scale band gaps. A shortcoming of this principle was identified early in the context of acoustic sound shielding. Here, a phononic crystal would have to be several meters in size in order to shield environmental noise in the audible frequency range. To overcome this limitation several authors[24,25] proposed a class of sonic crystals that exhibit spectral band gaps with the lattice constant is several order of magnitude smaller than the relevant sonic wavelength. The key idea is to introduce local resonances in each unit cell by playing with the material composition. The interaction of a locally resonant mode and the

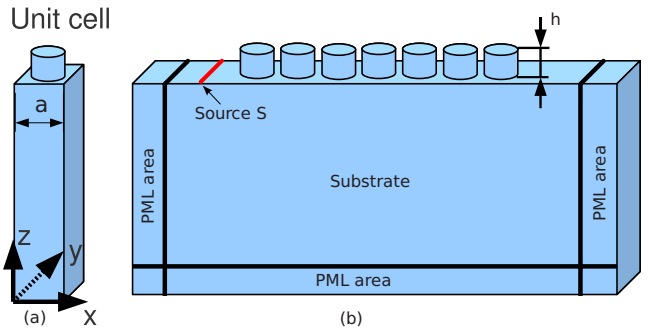

FIG. 1. (Color online) Phononic crystals composed of a square lattice array of cylindrical pillars on a substrate are considered. The lattice parameter is a and the pillars have height h and radius r. (a) The unit cell domain used for band structure calculations is meshed in three dimensions and Bloch-Floquet periodic boundary conditions are applied in both the x and the y direction. (b) The domain used for transmission computations has periodic boundary conditions along the y direction and a finite extent along the x direction. Perfectly matched layers are used to prevent reflexions from the domain boundaries. A line S generates waves propagation in the (x,y) plane, including surface acoustic waves.

bulk modes of the matrix can then open a low-frequency band gap.

In this paper, we add local acoustic resonances to a semi-infinite medium by considering a doubly periodic array of pillars on a surface.[26] The main effect observed is the possibility of finding a low-frequency gap for acoustic waves guided by the surface. The band gap can exist below the sound cone for the substrate and overcomes the acoustic loss issue usually observed with Bragg-based phononic crystals. Surface acoustic waves within Bragg regime can be obtained by drilling holes in a matrix[12,14] and the dispersion of the guided waves remains close to the upper part of the sound cone. We specifically consider in this paper a structure constituted by a square array of cylindrical silicon pillars on the surface of a semi-infinite silicon substrate. The numerical results presented here are thus related to the case of silicon, but the main conclusions should remain valid for other materials and compositions as well.

II. MODEL AND METHOD OF CALCULATION

As illustrated in Fig. 1, we consider a square lattice array of cylindrical pillars on the surface of semi-infinite substrate. The z axis is chosen to be perpendicular to the surface and parallel to the cylinder axis. The lattice parameter of the phononic crystal is a. The filling fraction is defined as $F=\pi r^2/a^2$, where r is the radius of the cylinder. The height of the cylinders is h. Dispersion curves are calculated for the infinite system by using a finite element method, in which only the unit cell is meshed and Bloch-Floquet conditions are implemented via periodic boundary conditions.[15] A three-dimensional mesh is used and the structure is assumed to be infinite and periodic in both the x and y directions [Fig. 1(a)]. A phase relation is applied on the lateral sides of the mesh, defining boundary conditions between adjacent cells. This phase relation is related to the Bloch wave number of the modes of the periodic structure. By varying the wave vector in the first Brillouin zone and solving an eigenvalue problem, the eigenfrequencies are obtained. The eigenvectors represent the modal displacement fields.

For transmission calculations, the model depicted in Fig. 1(b) is used. An incident surface acoustic wave with a specific polarization (u_x,u_z,u_y) is modeled by applying a line source vibrating on the surface. We apply in the y direction a periodic boundary condition that renders the line source infinitely long. The line source thus generates waves propagating in the (x,z) plane with uniform phase fronts along the y direction. In the far field of the source, the generated waves can be either bulk waves propagating away inside the substrate or surface waves propagating along the surface in the x direction. We assume that few wavelength from the source, displacements at the surface are only caused by surface waves and not by bulk waves. To prevent reflections caused by the scattering of waves from the domain boundaries, perfectly matched layers (PMLs)[27] are applied as illustrated in Fig. 1(b). PMLs have the property that the mechanical disturbances are gradually absorbed in the layers before they can reach the outer boundaries.[28] Indeed, we can write the governing equation as

$$\frac{1}{\gamma_j}\frac{\partial T_{ij}}{\partial x_j} = -\rho\omega^2 u_i, \tag{1}$$

where ρ is the mass density of the material and ω is the angular frequency. Summation over repeated indices is implicitly assumed. T_{ij} is the stress tensor, the u_i are the displacements, and the x_j are the coordinates $(x_1=x,\ x_2=y,\ x_3=z)$. Function $\gamma_j(\mathbf{r})$ is the artificial damping along axis x_j at an arbitrary position $\mathbf{r}$ inside the PML. As PMLs are added to attenuate acoustic waves propagating in the (x,z) plane, only γ_1 and γ_3 are different from 1. γ_x is for instance given by

$$\gamma_1(x_1) = 1 - i\sigma_1(x_1 - x_l)^2, \tag{2}$$

where x_l is the coordinate of the interface between the regular domain and the PML and σ_1 is a suitable constant. There is no damping outside the PMLs and here $\gamma_j=1$ is assumed. A suitable thickness of the PML as well as the value of σ_j must be found by trial calculations such that mechanical disturbances are absorbed before reaching the outer boundaries. However, the absorption variation must also be sufficiently slow so that reflections occurring at the interface between the regular domain and the PML are kept minimal. The mechanical stresses T_{ij} further depend on the strains as

$$T_{ij} = C_{ijkl}S_{kl}, \tag{3}$$

where the C_{ijkl} are the elastic stiffness constants. Strains are related to the displacements according to

$$S_{ij} = \frac{1}{2}\left(\frac{1}{\gamma_j}\frac{\partial u_i}{\partial x_j} + \frac{1}{\gamma_i}\frac{\partial u_j}{\partial x_i}\right). \tag{4}$$

III. RESULTS AND DISCUSSION

Before starting to discuss the results, we wish to outline that the geometry we consider has a strong relation to asym-

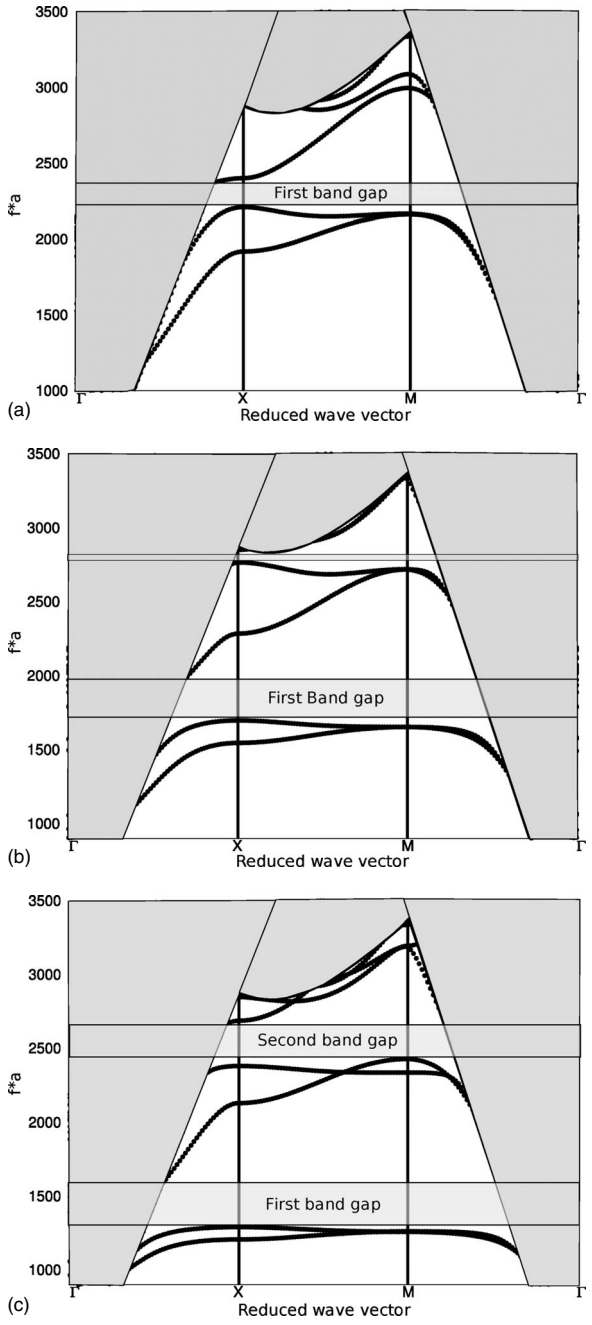

FIG. 2. Band structure of a phononic crystal composed of cylindrical silicon pillars on a silicon substrate, calculated along high symmetry directions of the first irreducible Brillouin zone. The lattice parameter is a and the filling fraction $F=0.28$. the relative height of the cylinders h/a equals (a) 0.3, (b) 0.4, and (c) 0.5. The gray region represents the sound cone of the substrate. The sound line limiting the sound cone is given by the smallest phase velocity in the substrate for every propagation direction.

metric photonic crystal slabs but is conversely quite different from phononic crystal slabs, which may not be obvious at first sight. Phononic crystals slabs surrounded by vacuum provide naturally a perfect confinement of waves in the vertical direction and their in-plane band gaps are similar to those of three-dimensional phononic crystals,[24] but those band gaps are very sensitive to the existence of additional

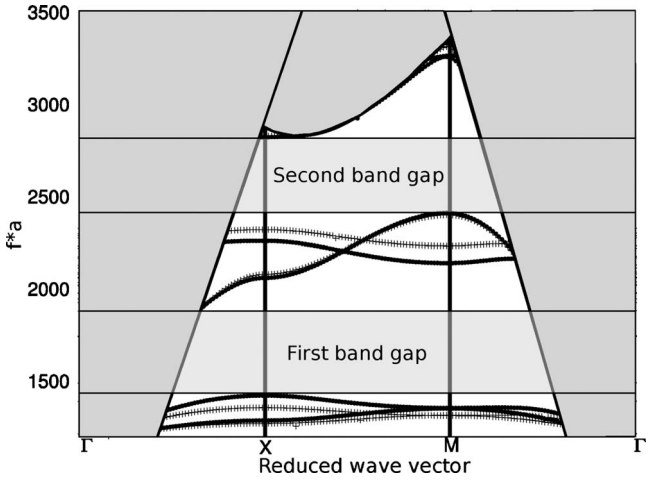

FIG. 3. Band structure of a phononic crystal composed of cylindrical silicon pillars on a silicon substrate, calculated along high symmetry directions of the first irreducible Brillouin zone. The lattice parameter is a and the relative height of the cylinders $h/a=0.5$. Two values of the filling fraction are compared, $F=0.35$ (dotted line) and $F=0.5$ (solid line).

branches originating from the finite thickness of the slab.[15] Conversely, as discussed e.g., by Johnson *et al.*,[29] there exists in photonic crystal slabs a continuum of radiation states that are extended infinitely in the region outside the slab. Guided modes, which are states localized to the plane of the slab, can only exist in the regions of the band diagram that are outside the light cone. Similarly, since the array of pillars we consider sits on top of a semi-infinite medium, the continuum of radiation states in this medium forms a sound cone. Guided acoustic waves localized to the pillar array and the immediate vicinity of the substrate surface can only exist in the regions of the band diagram that are outside the sound cone. The reason why we speak of a phononic crystal for periodic arrays of pillars on a surface is that they possess band gaps for guided waves. In the following, we consequently restrict our definition of band gaps to a range of frequencies, in which no guided modes exist.

Obviously, the first parameter which can play an important role is the height of the pillars. In order to investigate its influence, we have calculated band structures for the guided modes of the phononic crystal depicted in Fig. 1(a). Propagation is in the (x,y) plane, and band structures are generated along the high symmetry axes of the first Brillouin zone. Both the substrate and the pillars are made of [100] silicon. A low filling fraction $F=0.28$ $(r/a=0.3)$ and different relative heights of the cylinders $(h/a=0.3,\ 0.4$ and $0.5)$ were considered in Fig. 2. These particular choices for h/a ensure the existence of several absolute band gaps for guided modes. For $h/a=0.3$, one band gap appears for $fa=2200-2400$ m/s. The gray region on the band structure is the sound cone representing the radiative zone of the silicon substrate. The sound line limiting the sound cone is computed from the smallest phase velocity in the substrate as a function of the propagation direction. Due to the anisotropy of bulk acoustic phonon propagation in silicon, the sound line varies continuously along the XM direction of the first Brillouin zone. In practice, we have applied a linear variation

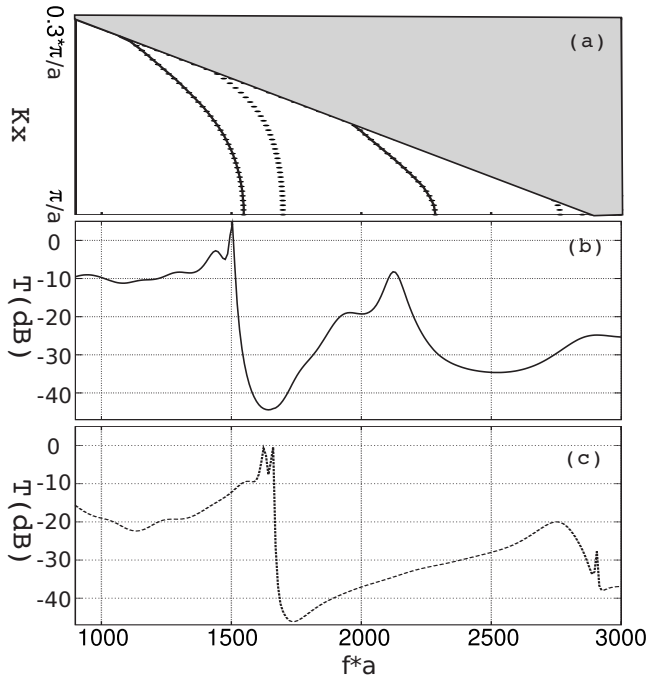

FIG. 4. Transmission of surface waves through 7 rows of a square-lattice phononic crystal composed of cylindrical silicon pillars on a silicon substrate. The filling fraction $F=0.28$ and the relative height is $h/a=0.4$. (a) Band structure for surface guided waves propagating along the ΓX direction. The first and the third bands are shown with solid lines, while the second and the fourth bands are shown with dotted lines. (b) Computed transmission spectrum with a sagittally polarized excitation line source. (c) Computed transmission spectrum with a shear horizontally polarized excitation line source. Transmissions represent an average of all displacement components, $|u_x|+u_z|+|u_y|$, as a function of frequency. The average is collected along a line located after the seventh period of pillars.

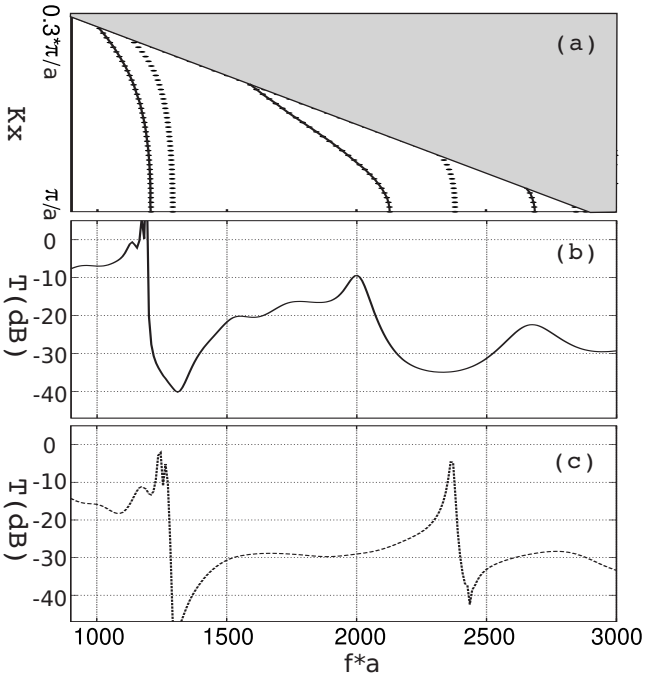

FIG. 5. Transmission of surface waves through 7 rows of a square-lattice phononic crystal composed of cylindrical silicon pillars on a silicon substrate. The filling fraction $F=0.28$ and the relative height is $h/a=0.5$. (a) Band structure for surface guided waves propagating along the ΓX direction. (b) Computed transmission spectrum with a sagittally polarized excitation line source. (c) Computed transmission spectrum with a shear horizontally polarized excitation line source.

from point X, where the sound line is limited by the shear horizontal wave with velocity $\sqrt{\frac{C_{44}}{\rho}}$, to point M, where the sound line is limited by the quasishear horizontal wave with velocity $\sqrt{\frac{C_{11}-C_{12}}{2\rho}}$. This approximation is very close the exact dispersion of the sound line in silicon when varying the propagation direction from the [100] to the [110] crystallographic axes.

When the height of the pillars is increased, the bands shift down toward low frequencies and band gaps show up. For $h/a=0.4$, we find two band gaps extending, respectively, from $fa=1700$ to 1970 m/s and a very narrow band gap appearing around $fa=2800$ m/s. For $h/a=0.5$, the first band gap shifts down to a central frequency $fa=1450$ m/s and a relative bandwidth of 22%. A wider second band gap appears around $fa=2550$ m/s with a 10% relative bandwidth. In Fig. 2, the period and the filling fraction are kept fixed, which clearly shows that the origin of the band gaps is not related to Bragg interference, as with classic phononic crystals, but is rather the result of resonant modes of the structure. Indeed, if h/a is smaller than 0.3, the discrete acoustic vibration modes of the pillars appear at frequencies within the sound cone and thus radiate into the bulk. However, when h/a is increased, the acoustic modes of the pillars shift down in frequency. They are then in a position to interact and form collective propagating surface modes, whereby acoustic energy can be guided along the surface of the substrate. Concurrently, this interaction opens band gaps inside which guided surface acoustic waves are forbidden to propagate. The band gaps shown in Fig. 2 are complete and omnidirectional for guided modes at the surface of the substrate. Such guided waves exist only under the sound cone such as, for instance, the Rayleigh surface wave of the homogeneous surface. This means that when a standard Rayleigh surface wave propagating on the free surface of the substrate is incident on the pillar array, it will be either converted to the existing surface-pillar modes at the same frequency, or reflected from the array if the frequency is within a band gap for guided waves. Naturally, a fraction of the surface wave energy can be converted to radiation modes of the substrate at the phononic crystal boundary in both cases, but this does not preclude that no energy is propagated along the surface within a band gap for guided waves.

Usually, the filling fraction F of a phononic crystal is an important parameter in the process of opening band gaps and controlling their bandwidths. We plot in Fig. 3 the band structure for the two values $F=0.38$ and 0.5. The relative height h/a is fixed to 0.5. We observe a relative widening of the two band gaps for guided waves for both values of F, as compared to $F=0.28$ in Fig. 2. Indeed, when the filling fraction is increased, or the space between adjacent pillars is reduced, the interaction between locally resonant modes can be enhanced through surface coupling and can lead to wider

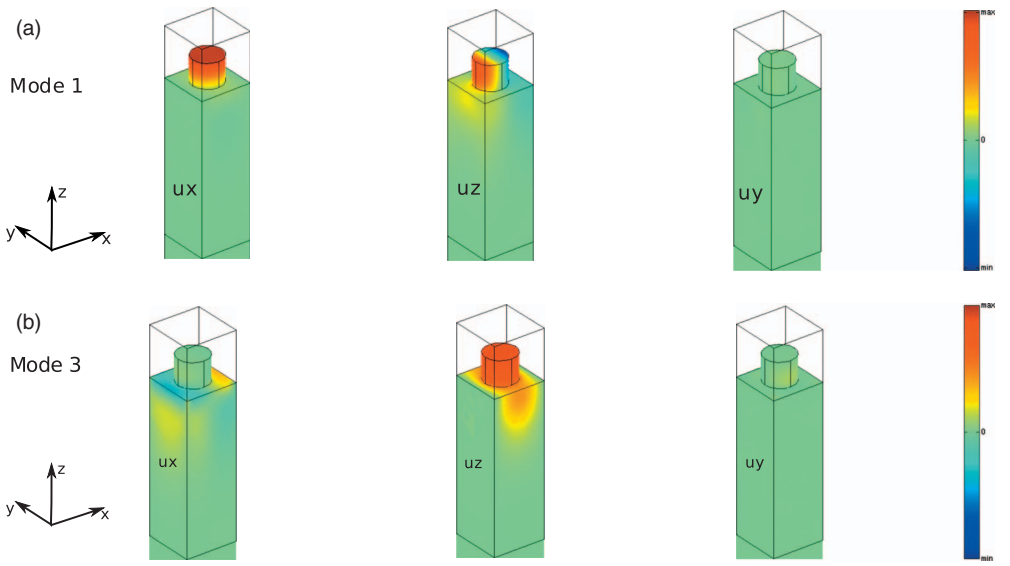

FIG. 6. (Color) Eigenmode of mode 1 and mode 3 analysis close to the point X of the Brillouin zone. This represent the displacement field of the three component *ux* and *uz* and *uy*. these modes have mostly in-plane polarization

band gaps. The central frequency and the relative bandwidth of the first band gap are, respectively, $fa=1667$ m/s and 28.7% for $F=0.38$, and $fa=1630$ m/s and 33.8% for $F=0.5$. The second band gap is bound up by the sound line and has the same central frequency and relative bandwidth for both values of F, namely $fa=2611$ m/s and 16%. We observe that the second and the fourth bands are more sensitive to the filling fraction and present a negative slope indicating negative group velocity along the XM direction. This could lead to unusual wave phenomena such as negative refraction or the superlens effect observed in phononic metamaterial structures.[30,31] These effects are however outside the scope of the present paper.

Transmission spectra were next computed for propagation along the x direction, using the three dimensional domain depicted in Fig. 1(b). The domain is finite along x with seven rows of pillars sandwiched between the incoming and outgoing media. As discussed in Sec. II, the structure is infinite and periodic along y. A line source is applied on the surface of the silicon substrate just in front of the phononic crystal. The line source vibrates at a monochromatic frequency and can have two different polarizations: either (i) (u_x, u_z) sagittal displacements, which can excite the Rayleigh surface wave of the homogeneous surface or (ii) u_y transverse displacements which can be considered as a shear horizontal wave source. It is well known that for most elastic materials the free surface (i.e., without phononic crystal) does not support the propagation of the shear horizontal surface wave; this is in particular the case of silicon. Nevertheless, the periodic array of pillars can support surface modes with such a polarization, as discussed in the following.

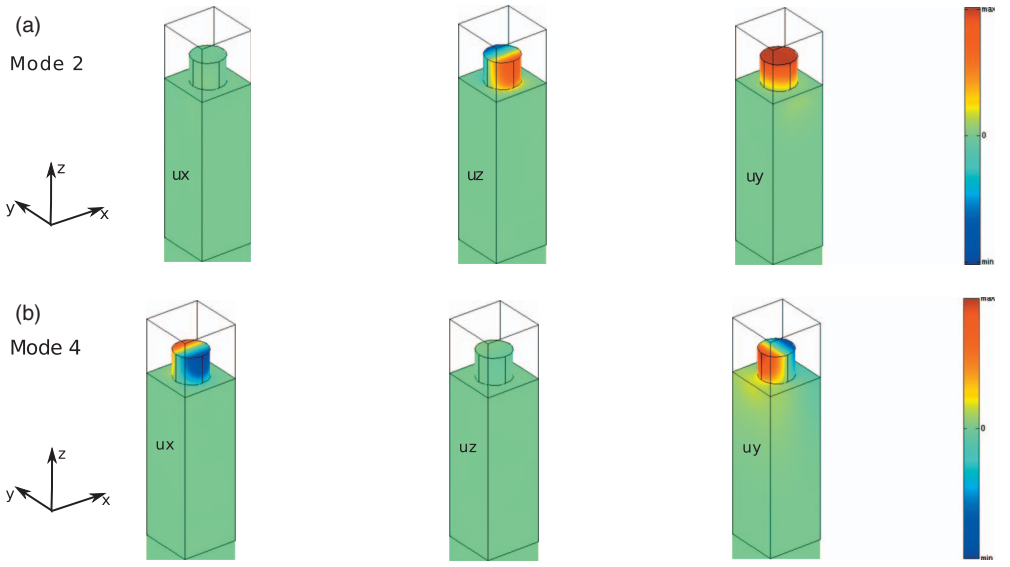

FIG. 7. (Color) Same as Fig. 6 for mode 2 and mode 4, these modes have mostly sagittal polarization with transverse propagation.

Figures 4 and 5 display the computed transmissions for the sagittal and the shear horizontal line sources. The filling fraction is fixed to $F=0.28$ and the relative height of the pillars is $h/a=0.4$ and 0.5, respectively. Transmissions are computed for the ΓX direction of the band structures which are added to Figs. 4 and 5 to help with the interpretation of the results. In Fig. 4(a), the band structure shows two band gaps extending from $fa=1700$ to 2000 m/s, and from $fa=2350$ to 2700 m/s, respectively. The transmission in Fig. 4(b) is for the total displacement, but is however related to the sagittal (ux,uz) excitation. Two attenuation frequency ranges are apparent, corresponding to the first and the third band limits in the band structure. The transmission in Fig. 4(c) is related to the transverse u_y excitation and shows a resonance around $fa=1600$ m/s and a damped resonance around $fa=2700$ m/s, that are related to the second and fourth bands of the band structure, respectively.

This effect is even more pronounced when $h/a=0.5$ as apparent in Fig. 5. The band structure of Fig. 5(a) has five bands delimiting the stop bands and pass bands. The computed transmission for the sagittal excitation line source in Fig. 5(b) shows two attenuation regions limited by the first, the third and the fifth bands. The computed transmission for the shear horizontal line source in Fig. 5(c) displays two small pass bands around $fa=1300$ and 2375 m/s. The second and the fourth branches are deaf to the sagittal source while first, third and fifth bands are deaf to the shear horizontal source. We can observe also that the shape of the transmission for the shear horizontal source around the frequencies where the second and fourth bands reach the X point is typical of a linear response function proportional to $1/(f_0^2-f^2)$, when a wave with frequency f interacts with a medium supporting a localized excitation with frequency f_0. Such an effect is manifested for instance in the electromagnetic frequency response of materials with optical resonances.

In order to corroborate the previous observations, we plot in Figs. 6 and 7 the modal displacements of the first and the third bands, and on the second and fourth bands, respectively. The wave vector k_x selected for these illustrations is close to the X point of the first Brillouin zone. We emphasize that the acoustic energy is mostly distributed between u_x and u_z for the eigenmodes in Fig. 6. Those modes have mostly sagittal polarization. The displacement u_y is not equal to zero but is very small in comparison. Note that the same scale has been used for all displacements. This observation explains the significant transmission magnitude for the first and the third bands for the sagittal source.

As Fig. 7 shows, the acoustic energy is mostly distributed between u_z and u_y for the second band and between u_x and u_y for the fourth band. We observe that the u_z displacement for the second band and the u_x displacement for the fourth band have an antisymmetric character with respect to the sagittal mid plane (x,z) of the structure. When a sagittal excitation is applied that is symmetric with respect to the same midplane, it is obvious that energy cannot be transferred to the second and the fourth bands. This explains the absence of signature of those modes in the transmission spectra with the sagittally polarized source. Conversely, the u_y displacement is symmetric with respect to the sagittal mid plane and can thus be excited by the shear horizontally polarized source.

IV. CONCLUSION

In this paper, we have studied theoretically the behavior of locally acoustic resonances of a periodic array of cylindrical pillars deposited on a semi-infinite substrate. We have calculated the band structure of the periodic medium and the transmission through a finite length array of pillars by using finite element method. With an appropriate choice of the geometrical parameters, we have shown that this structure supports surface propagating modes in the nonradiative region of the substrate, outside the sound cone. Especially, an in-plane polarized surface wave and a transverse surface wave that do not exist on the homogeneous surface are found. In addition, the band structure of the guided modes defines band gaps that appear at frequencies markedly lower than those expected from the Bragg condition. Those band gaps refer to a range of frequencies, in which no guided modes exist. We identify them as originating from local resonances of the individual cylindrical pillars and show their dependence with the geometrical parameters of the array, and in particular with the height of the pillars. The transmission of surface acoustic waves across a finite array of pillars shows the signature of the locally resonant band gaps for surface modes and their dependence on the symmetry of the source and its polarization.

ACKNOWLEDGMENTS

Financial support by the CNRS/JST joint project and the Agence Nationale de la Recherche under Grant No. ANR-09-BLAN-0167-07 are gratefully acknowledged.

[1] M. M. Sigalas and E. N. Economou, Solid State Commun. **86**, 141 (1993).
[2] M. S. Kushwaha, P. Halevi, L. Dobrzynski, and B. Djafari-Rouhani, Phys. Rev. Lett. **71**, 2022 (1993).
[3] T. Miyashita, Meas. Sci. Technol. **16**, R47 (2005).
[4] I. E. Psarobas, Z. Kristallogr. **220**, IV (2005).
[5] An exhaustive list of references on phononic crystals can be found at http://www.phys.uoa.gr/phononics/PhononicDatabase.html.
[6] E. Yablonovitch, Phys. Rev. Lett. **58**, 2059 (1987).
[7] S. John, Phys. Rev. Lett. **58**, 2486 (1987).
[8] J. O. Vasseur, P. A. Deymier, B. Chenni, B. Djafari-Rouhani, L. Dobrzynski, and D. Prevost, Phys. Rev. Lett. **86**, 3012 (2001).
[9] A. Khelif, B. Djafari-Rouhani, J.-O. Vasseur, and P. A. Deymier, Phys. Rev. B **68**, 024302 (2003).
[10] Y. Tanaka and S. I. Tamura, Phys. Rev. B **58**, 7958 (1998).
[11] T.-T. Wu, Z.-G. Huang, and S. Lin, Phys. Rev. B **69**, 094301 (2004).
[12] T.-T. Wu, L.-C. Wu, and Z.-G. Huang, J. Appl. Phys. **97**, 094916 (2005).

[13] V. Laude, M. Wilm, S. Benchabane, and A. Khelif, Phys. Rev. E **71**, 036607 (2005).
[14] S. Benchabane, A. Khelif, J.-Y. Rauch, L. Robert, and V. Laude, Phys. Rev. E **73**, 065601(R) (2006).
[15] A. Khelif, B. Aoubiza, S. Mohammadi, A. Adibi, and V. Laude, Phys. Rev. E **74**, 046610 (2006).
[16] F.-L. Hsiao, A. Khelif, H. Moubchir, A. Choujaa, C.-C. Chen, and V. Laude, Phys. Rev. E **76**, 056601 (2007).
[17] S. Mohammadi, A. Eftekhar, A. Khelif, H. Moubchir, R. Westafer, W. Hunt, and A. Adibi, Electron. Lett. **43**, 898 (2007).
[18] S. Mohammadi, A. A. Eftekhar, A. Khelif, W. Hunt, and A. Adibi, Appl. Phys. Lett. **92**, 221905 (2008).
[19] S. Mohammadi, A. A. Eftekhar, W. Hunt, and A. Adibi, Appl. Phys. Lett. **94**, 051906 (2009).
[20] B. Bonello, C. Charles, and F. Ganot, Appl. Phys. Lett. **90**, 021909 (2007).
[21] I. El-Kady, R. H. Olsson, and J. G. Fleming, Appl. Phys. Lett. **92**, 233504 (2008).
[22] Y. Pennec, B. Djafari-Rouhani, H. Larabi, J. O. Vasseur, and A. C. Hladky-Hennion, Phys. Rev. B **78**, 104105 (2008).
[23] T.-C. Wu, T.-T. Wu, and J.-C. Hsu, Phys. Rev. B **79**, 104306 (2009).
[24] Z. Liu, X. Zhang, Y. Mao, Y. Y. Zhu, Z. Yang, C. T. Chan, and P. Sheng, Science **289**, 1734 (2000).
[25] C. Goffaux, J. Sánchez-Dehesa, A. Levy Yeyati, P. Lambin, A. Khelif, J. O. Vasseur, and B. Djafari-Rouhani, Phys. Rev. Lett. **88**, 225502 (2002).
[26] J. F. Robillard, A. Devos, I. Roch-Jeune, and P. A. Mante, Phys. Rev. B **78**, 064302 (2008).
[27] J.-P. Berenger, J. Comput. Phys. **114**, 185 (1994).
[28] Maria B. Dühring, V. Laude, and A. Khelif, J. Appl. Phys. **105**, 093504 (2009).
[29] S. G. Johnson, S. Fan, P. R. Villeneuve, J. D. Joannopoulos, and L. A. Kolodziejski, Phys. Rev. B **60**, 5751 (1999).
[30] M. Farhat, S. Enoch, S. Guenneau, and A. B. Movchan, Phys. Rev. Lett. **101**, 134501 (2008).
[31] A. Sukhovich, B. Merheb, K. Muralidharan, J. O. Vasseur, Y. Pennec, P. A. Deymier, and J. H. Page, Phys. Rev. Lett. **102**, 154301 (2009).